

Supporting Information

Lanthanide-MOFs as multi-responsive photoluminescence sensor for sensitively detecting Fe^{3+} , $\text{Cr}_2\text{O}_7^{2-}$ and nitrofuran antibiotics

Jingjuan Feng,^{a#} Cunding Kong,^{a#} Yunhui Chen,^a Peipei Cen,^{*b} Yi Ding,^a Yan Guo,^a Fengyuan Zhang^b and Xiangyu Liu^{*a}

^a State Key Laboratory of High-efficiency Utilization of Coal and Green Chemical Engineering, National Demonstration Center for Experimental Chemistry Education, College of Chemistry and Chemical Engineering, Ningxia University, Yinchuan 750021, China.

^b College of Public Health and Management, Ningxia Medical University, Yinchuan 750021, China.

These authors contributed equally to this work.

***Corresponding author**

Prof. Dr. Xiangyu Liu

E-mail: xiangyuliu432@126.com

***Corresponding author**

Dr. Peipei Cen

E-mail: 13895400691@163.com.

Contents:

Fig. S1 View of the complexes **1-4** molecular structure with thermal ellipsoids drawn at 50% probability level (Eu cyan, Gd green, O red, N blue, C grey, H light grey).

Fig. S2 (a) The coordination environment of Gd^{3+} in **2**; (b) the coordination modes of pta^{2-} in **2**; (c) the dinuclear $[\text{Gd}_2(\text{COO})_2]$ cluster; (d) a view of the 3D structure of **2**. (Gd cyan, O red, N blue, C grey, hydrogen atoms are omitted for clarity).

Fig. S3 (a) Layer structure and (b) 3D structure of **2**.

Fig. S4 (a) The coordination environment of Gd^{3+} in **4**; (b) the coordination modes of pta^{2-} in **4**; (c) the dinuclear $[\text{Gd}_2(\text{COO})_2]$ cluster; (d) a view of the 2D structure of **4**. (Gd cyan, O red, N blue, C grey, hydrogen atoms are omitted for clarity).

Fig. S5 (a) Layer structure and (b) 2D structure of **4**.

Fig. S6 The simulated and experimental PXRD patterns of complexes **1**, **2** (a) and complexes **3**, **4** (b).

Fig. S7 TG spectra of **1** and **3**.

Fig. S8 Solid-state fluorescence spectrum of H_2pta .

Fig. S9 Solid-state fluorescence spectrum of **3**.

Fig. S10 luminescence intensity at 315 nm (excitation wavelength) of **3** dispersed in water with the addition of different ions (0.03 M) (Zn^{2+} , Pb^{2+} , Ni^{2+} , Co^{2+} , Na^+ , Cu^{2+} , Cd^{2+}) and Fe^{3+} incorporated systems (0.01M).

Fig. S11 (a), (b) and (c) Luminescence spectrum of **3** in Ethanol, acetonitrile and methanol solutions with Fe^{3+} at different concentrations; (d), (e) and (f) plots of relative luminescence intensity vs. Fe^{3+} concentration.

Fig. S12 (a), (b) and (c) Luminescence spectrum of **3** in Ethanol, acetonitrile and methanol solutions with Cu^{2+} at different concentrations; (d), (e) and (f) plots of relative luminescence intensity vs. Cu^{2+} concentration.

Fig. S13 (a) and (b) Luminescence spectrum of **3** in DMF and DMA solutions with Fe^{3+} at different concentrations; (c) and (d) plots of relative luminescence intensity vs. Fe^{3+} concentration.

Fig. S14 (a) and (b) Luminescence spectrum of **3** in DMF and DMA solutions with Cu^{2+} at different concentrations; (c) and (d) plots of relative luminescence intensity vs. Cu^{2+} concentration.

Fig. S15 (a) Luminescent intensity of **3** treated with 0.01 M of various different anions in DMF; (b) luminescence intensity of **3** dispersed in DMF with the addition of different anions and $\text{Cr}_2\text{O}_7^{2-}$ incorporated systems; (c) luminescence spectrum of **3** in DMF solutions with $\text{Cr}_2\text{O}_7^{2-}$ at different concentrations; (d) a plot of relative luminescence intensity vs. $\text{Cr}_2\text{O}_7^{2-}$ concentration.

Fig. S16 (a) and (b) Luminescence spectrum of **3** in aqueous solutions with $\text{Cr}_2\text{O}_7^{2-}$ and $\text{S}_2\text{O}_8^{2-}$ at different concentrations; (c) and (d) plots of relative luminescence intensity vs. $\text{Cr}_2\text{O}_7^{2-}$ and $\text{S}_2\text{O}_8^{2-}$ concentrations.

Fig. S17. Excitation spectra(blue) of **3** and UV-vis absorption spectra (black or red) for (a) Fe^{3+} aqueous solution; (b) $\text{Cr}_2\text{O}_7^{2-}$ in DMF (c) $\text{Cr}_2\text{O}_7^{2-}$ in DMA; (d) NFZ and NFT in DMF solution.

Fig S18. Fluorescence lifetimes of **3** (black curve) and **3**@ Fe^{3+} (10 μL , 0.01 mol/L) (blue curve).

Table S1. Selected crystallographic data for the complexes **1-4**.

Table S2. Selected bond lengths (\AA) and bond angles ($^\circ$) for **1-4**.

Table S3. Ions leading to fluorescence sensing for **3** in different organic solvents.

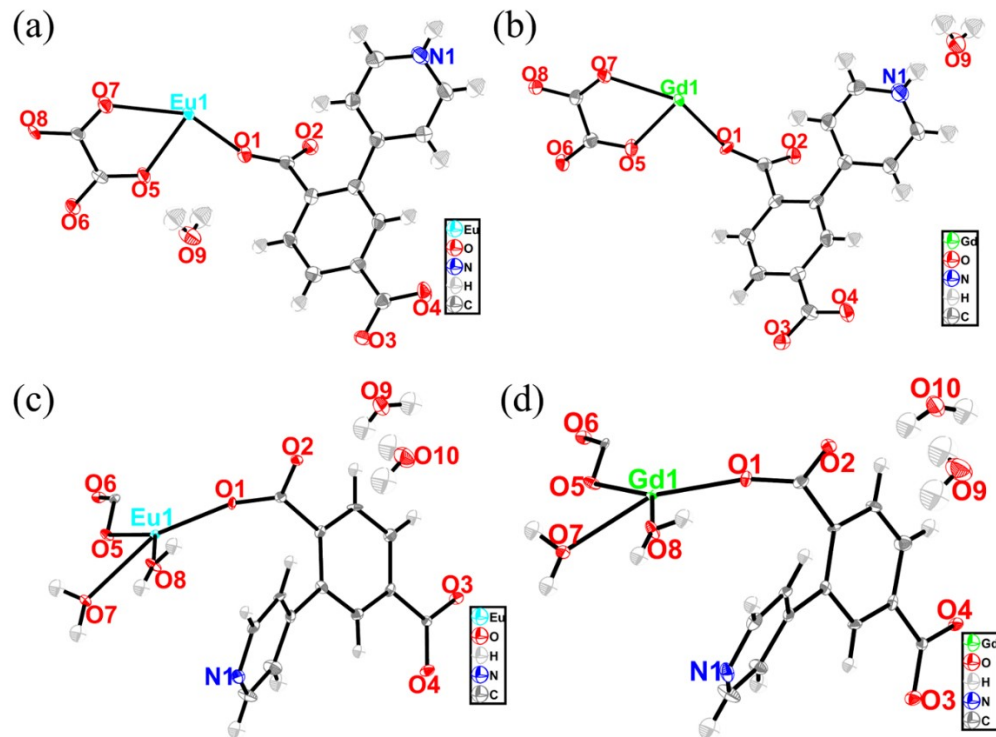


Fig. S1 View of the complexes **1-4** molecular structure with thermal ellipsoids drawn at 50% probability level (Eu cyan, Gd green, O red, N blue, C grey, H light grey)

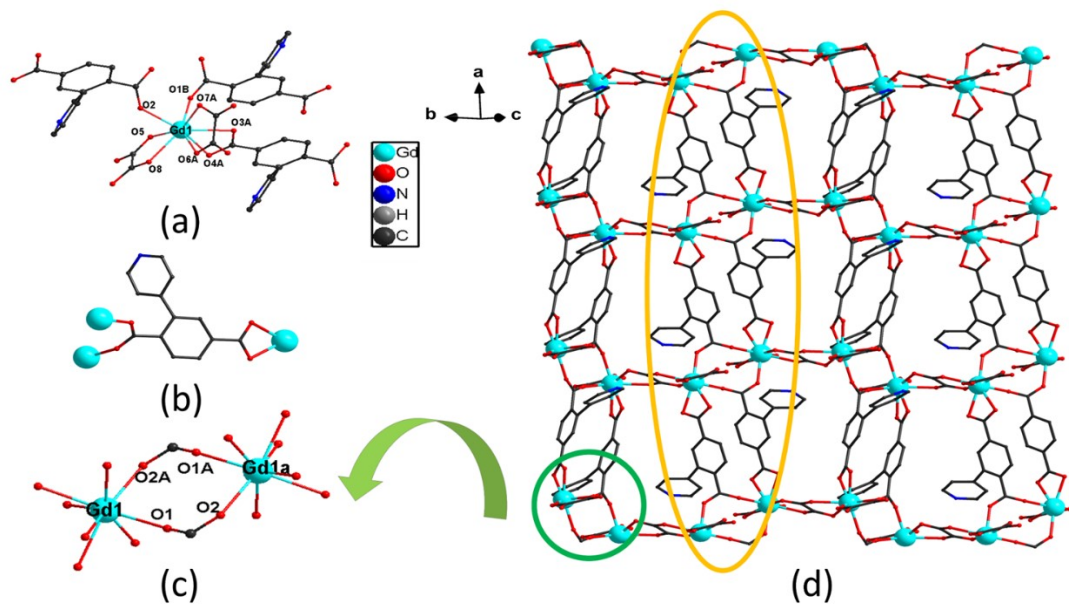


Fig. S2 (a) The coordination environment of Gd^{3+} in **2**; (b) the coordination modes of pta^{2-} in **2**; (c) the dinuclear $[\text{Gd}_2(\text{COO})_2]$ cluster; (d) a view of the 3D structure of **2**. (Gd cyan, O red, N blue, C grey, hydrogen atoms are omitted for clarity).

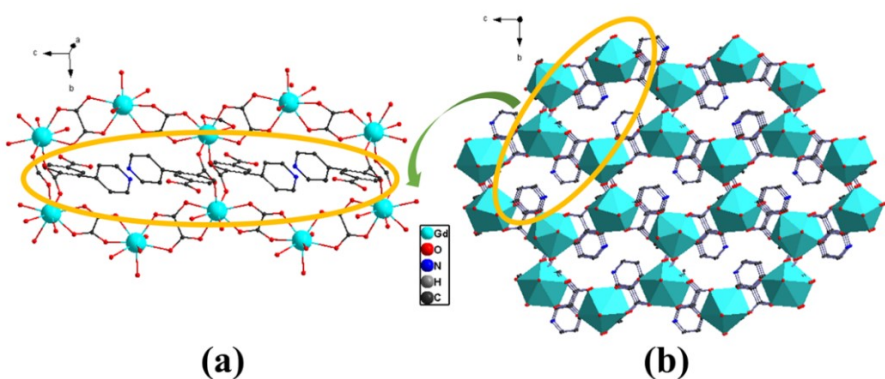


Fig. S3 (a) Layer structure and (b) 3D structure of 2.

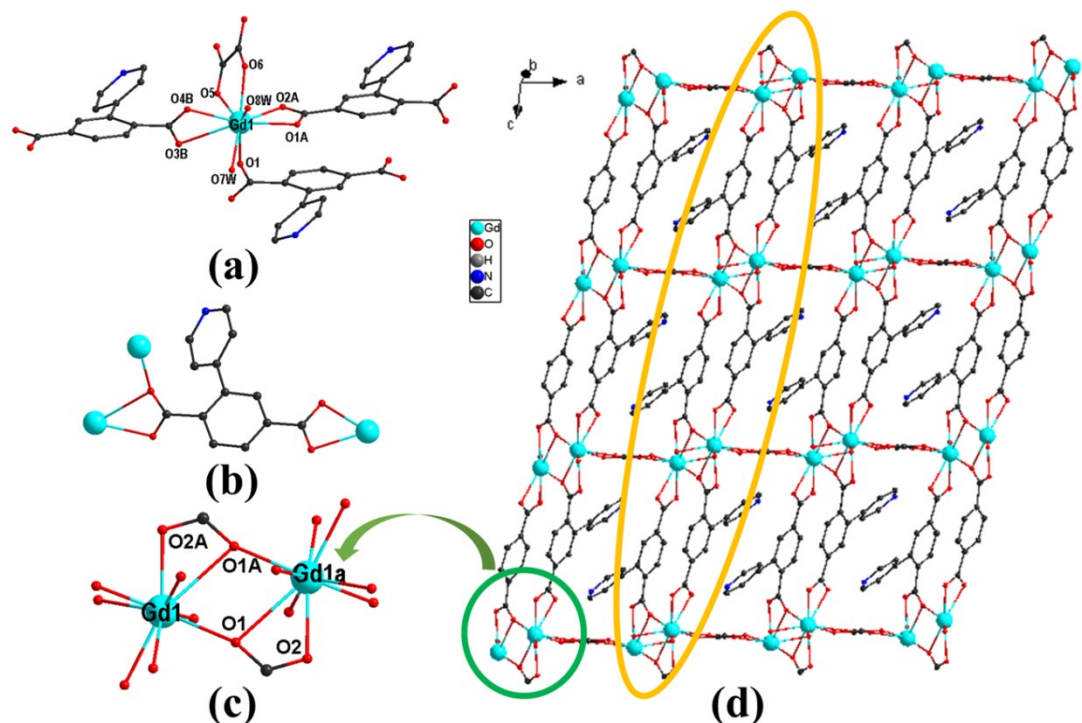


Fig. S4 (a) The coordination environment of Gd^{3+} in 4; (b) the coordination modes of pta²⁻ in 4; (c) the dinuclear $[\text{Gd}_2(\text{COO})_2]$ cluster ;(d) a view of the 2D structure of 4. (Gd cyan, O red, N blue, C grey, hydrogen atoms are omitted for clarity).

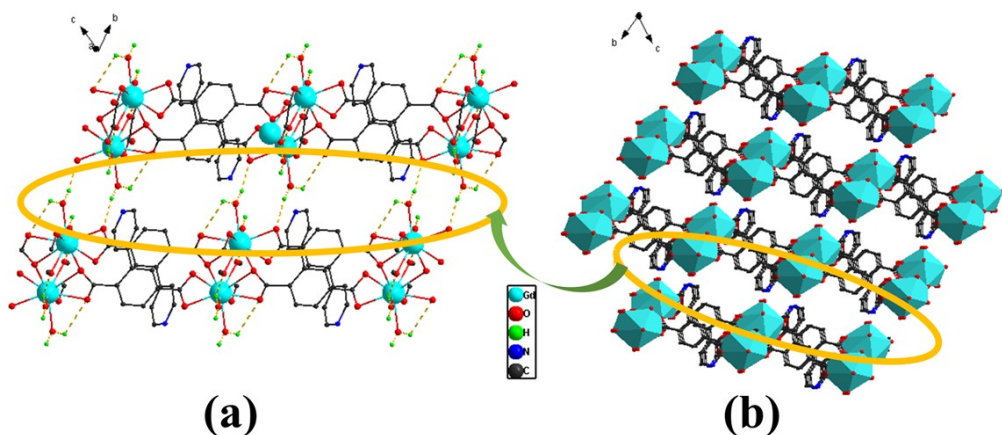


Fig. S5 (a) Layer structure and (b) 2D structure of **4**.

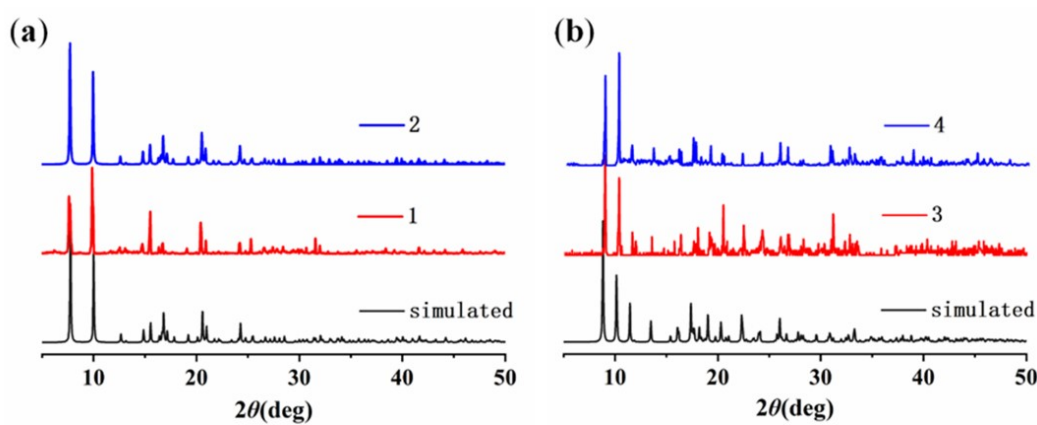


Fig. S6 The simulated and experimental PXRD patterns of complexes **1**, **2** (a) and complexes **3**, **4** (b).

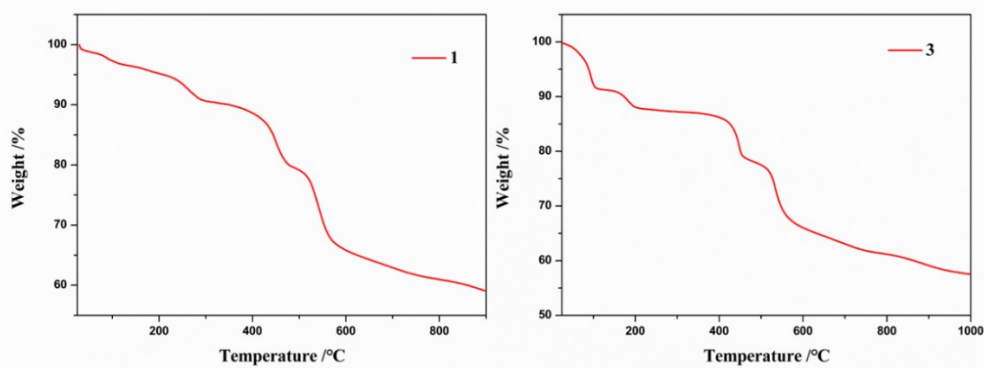


Fig. S7 TG spectra of **1** and **3**.

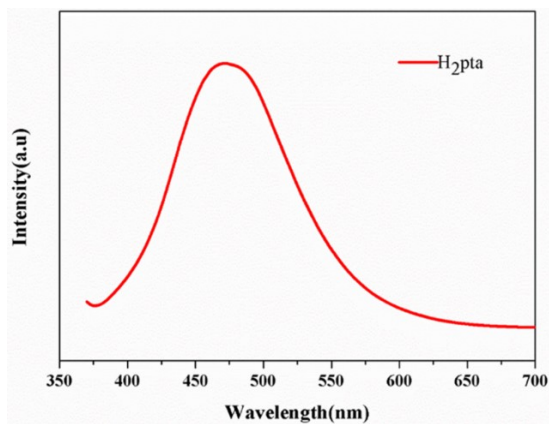


Fig. S8 Solid-state fluorescence spectrum of H_2pta .

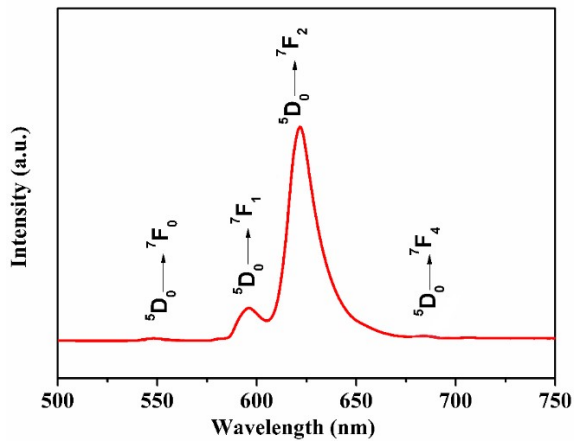


Fig. S9 Solid-state fluorescence spectrum of **3**.

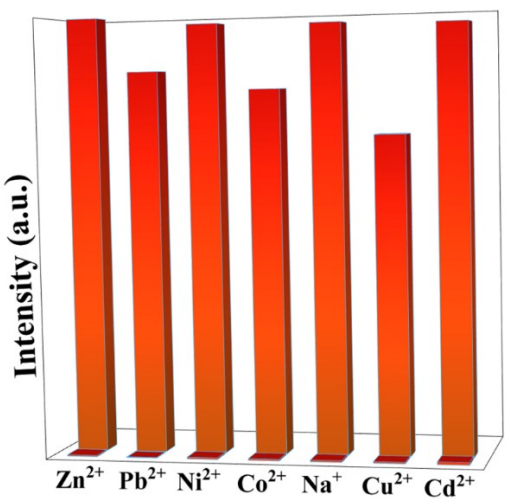


Fig. S10 luminescence intensity at 315 nm (excitation wavelength) of **3** dispersed in water with the addition of different ions (0.03 M) (Zn^{2+} , Pb^{2+} , Ni^{2+} , Co^{2+} , Na^+ , Cu^{2+} , Cd^{2+}) and Fe^{3+} incorporated systems (0.01M).

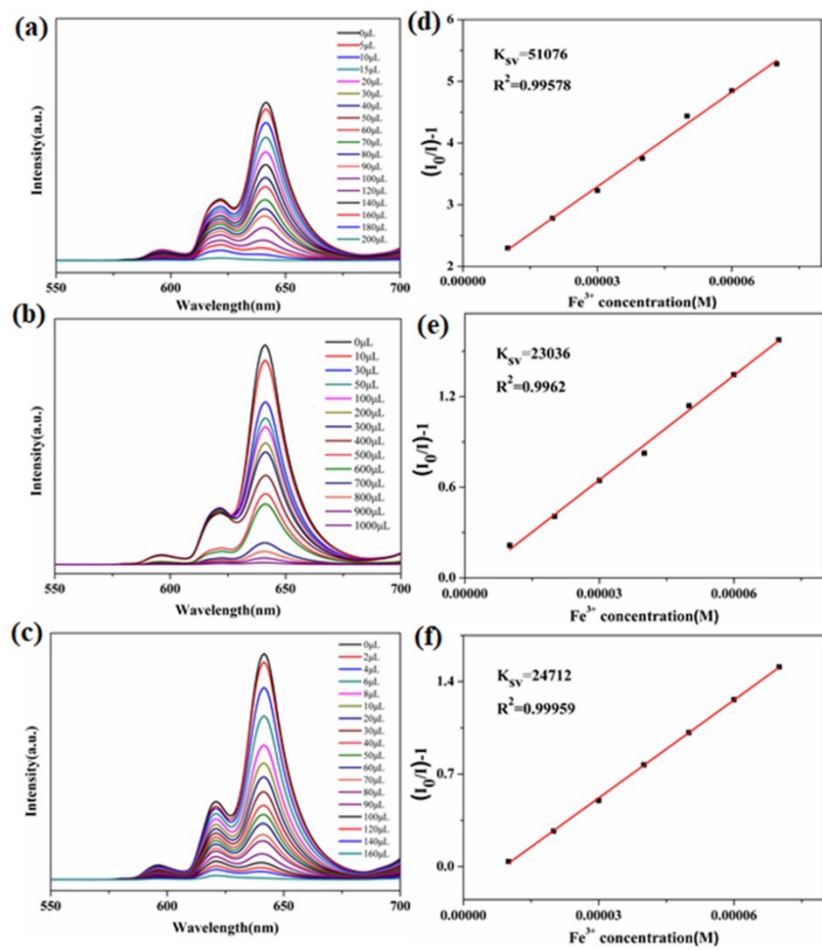


Fig. S11 (a), (b) and (c) Luminescence spectrum of **3** in Ethanol, acetonitrile and methanol solutions with Fe^{3+} at different concentrations; (d), (e) and (f) plots of relative luminescence intensity vs. Fe^{3+} concentration.

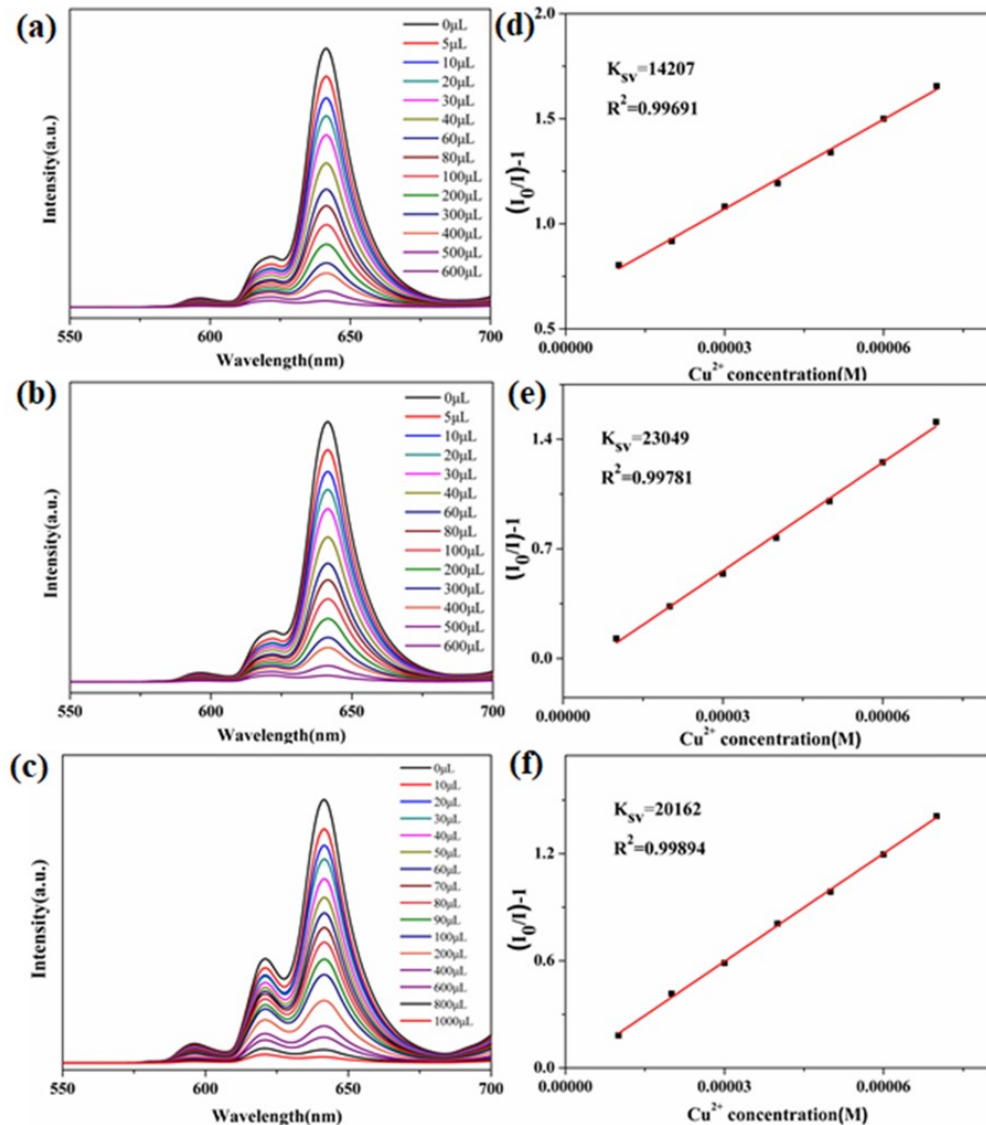


Fig. S12 (a), (b) and (c) Luminescence spectrum of **3** in Ethanol, acetonitrile and methanol solutions with Cu^{2+} at different concentrations; (d), (e) and (f) plots of relative luminescence intensity vs. Cu^{2+} concentration.

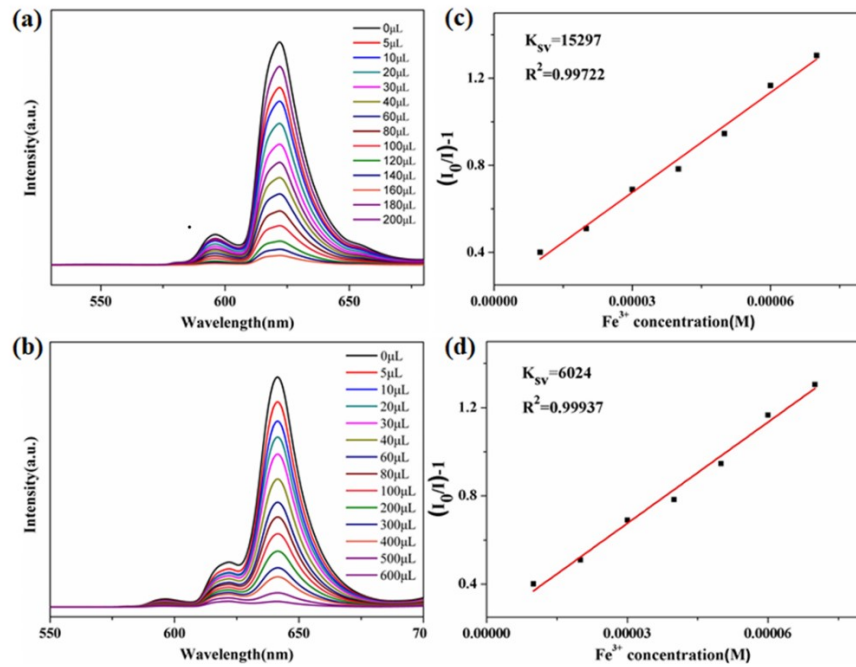


Fig. S13 (a) and (b) Luminescence spectrum of **3** in DMF and DMA solutions with Fe^{3+} at different concentrations; (c) and (d) plots of relative luminescence intensity vs. Fe^{3+} concentration.

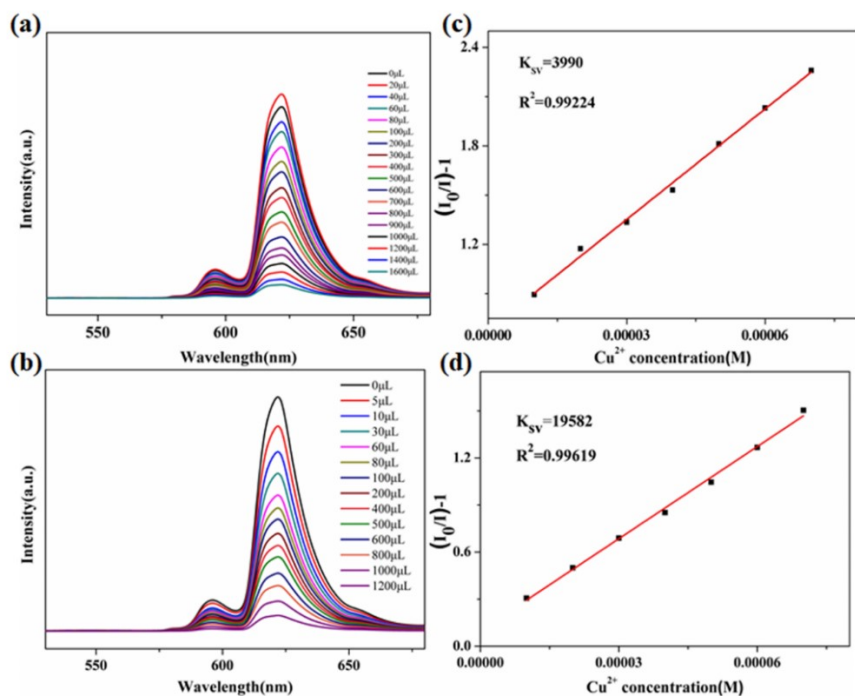


Fig. S14 (a) and (b) Luminescence spectrum of **3** in DMF and DMA solutions with Cu^{2+} at different concentrations; (c) and (d) plots of relative luminescence intensity vs. Cu^{2+} concentration.

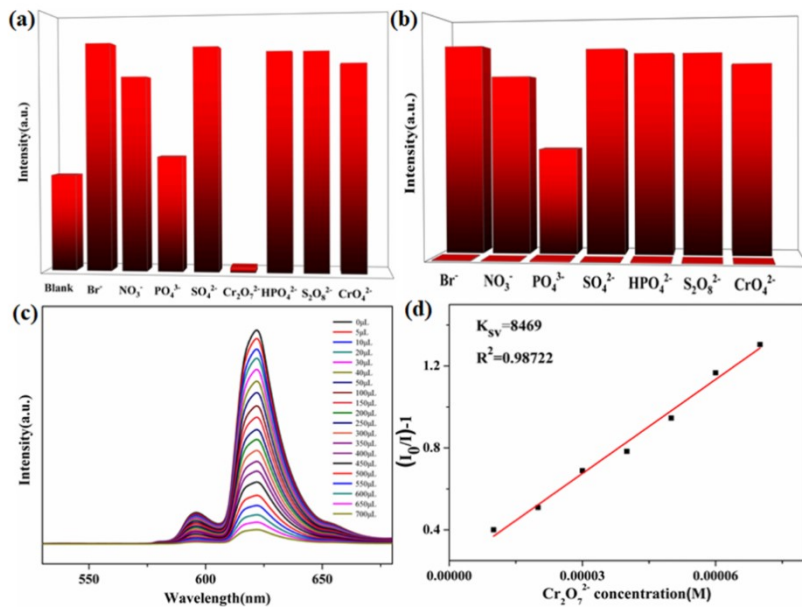


Fig. S15 (a) Luminescent intensity (315 nm: excitation wavelength) of **3** treated with 0.01 M of various different anions in DMF; (b) luminescence intensity of **3** dispersed in DMF with the addition of different anions and $\text{Cr}_2\text{O}_7^{2-}$ incorporated systems; (c) luminescence spectrum of **3** in DMF solutions with $\text{Cr}_2\text{O}_7^{2-}$ at different concentrations; (d) a plot of relative luminescence intensity vs. $\text{Cr}_2\text{O}_7^{2-}$ concentration.

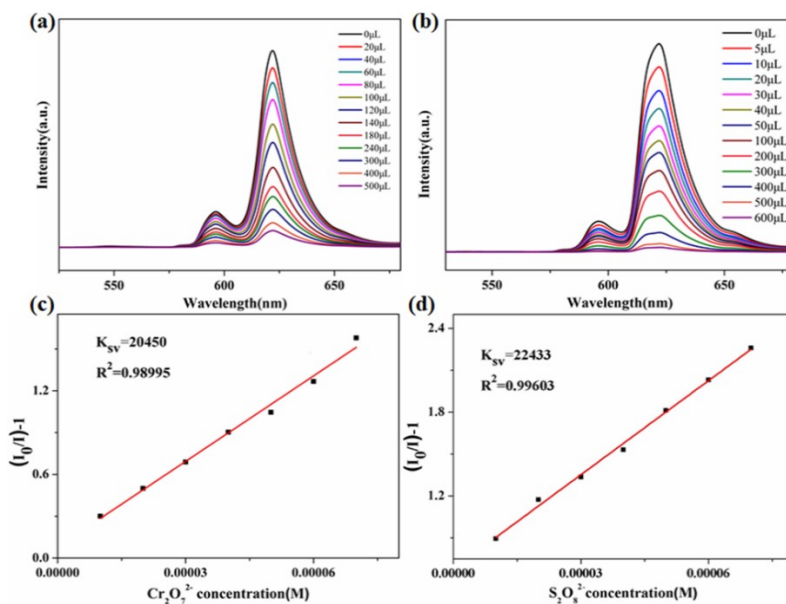


Fig. S16 (a) and (b) Luminescence spectrum of **3** in aqueous solutions with $\text{Cr}_2\text{O}_7^{2-}$ and $\text{S}_2\text{O}_8^{2-}$ at different concentrations; (c) and (d) plots of relative luminescence intensity vs. $\text{Cr}_2\text{O}_7^{2-}$ and $\text{S}_2\text{O}_8^{2-}$ concentrations.

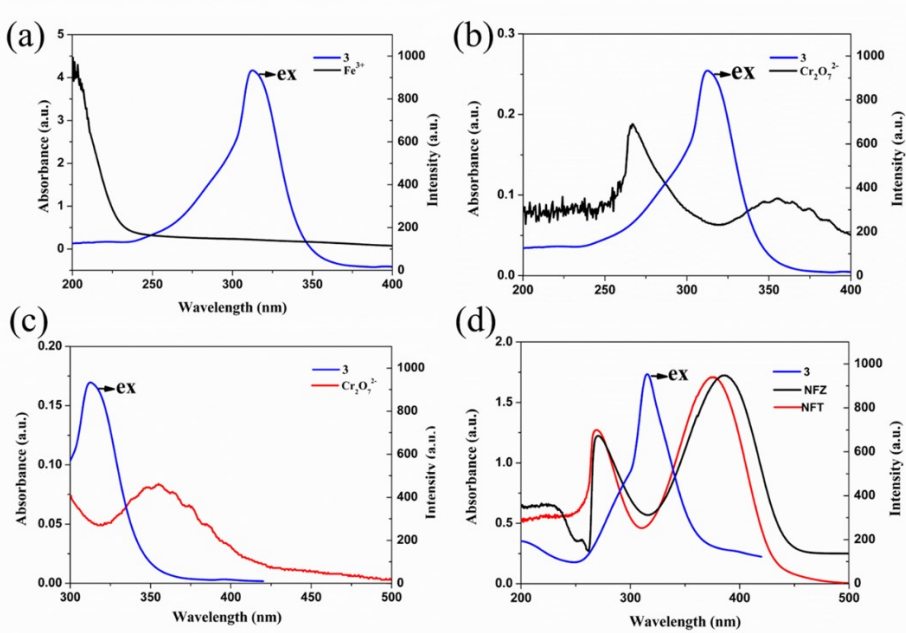


Fig. S17. Excitation spectra(blue) of **3** and UV-vis absorption spectra (black or red) for (a) Fe³⁺ aqueous solution; (b) Cr₂O₇²⁻ in DMF (c) Cr₂O₇²⁻ in DMA; (d) NFZ and NFT in DMF solution.

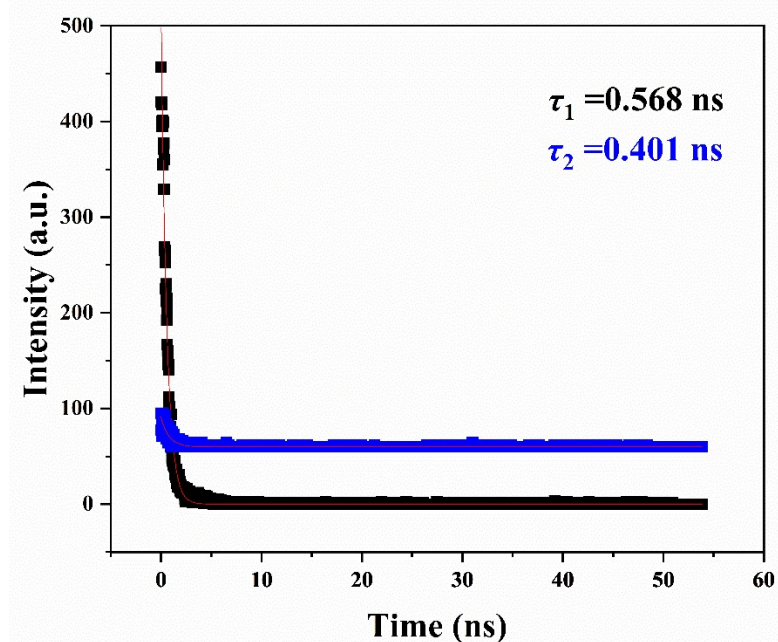


Fig S18. Fluorescence lifetimes of **3** (black curve) and **3**@Fe³⁺(10 μL , 0.01 mol/L) (blue curve).

Table S1. Selected crystallographic data for the complexes **1-4**.

	1	2	3	4
Empirical formula	C ₁₅ H ₁₀ EuNO ₉	C ₁₅ H ₁₀ GdNO ₉	C ₁₄ H ₁₅ EuNO ₁₀	C ₁₄ H ₁₅ GdNO ₁₀
Formula weight	500.20	505.49	509.23	514.52
Temperature	150K	150K	100 K	100K
Crystal system	monoclinic	monoclinic	triclinic	Triclinic
Space group	P2 ₁ /c	P2 ₁ /c	P-1	P-1
<i>a</i> (Å)	11.4603(3)	11.4466(3)	8.4877(7)	8.4519(5)
<i>b</i> (Å)	13.9922(4)	13.9709(4)	10.4777(12)	10.4464(8)
<i>c</i> (Å)	11.4697(4)	11.4477(3)	11.1966(10)	11.1686(6)
α (°)	90	90	64.866(10)	64.867(6)
β (°)	96.428(3)	95.931(3)	87.056(7)	87.068(5)
γ (°)	90	90	67.138(9)	67.318(6)
<i>V</i> (Å ³)	1827.65(10)	1820.91(8)	822.89(16)	816.17(10)
<i>Z</i>	4	4	2	2
<i>D</i> (g/cm ³)	1.818	1.844	2.055	2.094
<i>Mu</i> (mm ⁻¹)	25.008	24.002	3.868	4.120
<i>F</i> (0 0 0)	968	972	498.0	500
Unique reflections	3204	3193	3815	3799
Observed reflections	7381	6015	6915	6986
<i>R</i> _{int}	0.0425	0.0424	0.0369	0.0436
Final <i>R</i> indices [<i>I</i> >2σ(<i>I</i>)]	<i>R</i> ₁ = 0.0341 w <i>R</i> ₂ = 0.0812	<i>R</i> ₁ = 0.0370 w <i>R</i> ₂ = 0.0906	<i>R</i> ₁ = 0.0345 w <i>R</i> ₂ = 0.0604	<i>R</i> ₁ = 0.0342 w <i>R</i> ₂ = 0.0564
<i>R</i> indices (all data)	<i>R</i> ₁ = 0.0435 w <i>R</i> ₂ = 0.0858	<i>R</i> ₁ = 0.0461 w <i>R</i> ₂ = 0.0975	<i>R</i> ₁ = 0.0403 w <i>R</i> ₂ = 0.0632	<i>R</i> ₁ = 0.0403 w <i>R</i> ₂ = 0.0608
Goodness-of-fit on <i>F</i> ²	1.012	1.033	1.025	0.996

Table S2. Selected bond lengths (Å) and bond angles (°) for **1-4**.

Complex 1			
Eu(1)-O(1)	2.314(4)	O(2)-Eu(1)#1	2.375(5)
Eu(1)-O(2)#1	2.372(3)	O(3)-Eu(1)#2	2.481(5)
Eu(1)-O(3)#2	2.480(3)	O(4)-Eu(1)#2	2.416(5)
Eu(1)-O(4)#2	2.419(4)	O(6)-Eu(1)#4	2.425(5)
Eu(1)-O(5)	2.420(4)	O(8)-Eu(1)#4	2.415(5)
Eu(1)-O(6)#3	2.426(4)	O(1)-Eu(1)-O(4)#2	89.73(19)

Eu(1)-O(7)	2.402(4)	O(1)-Eu(1)-O(5)	76.84(12)
Eu(1)-O(8)#3	2.418(3)	O(1)-Eu(1)-O(6)#3	147.31(12)
O(1)-Eu(1)-O(2)#1	86.51(13)	O(1)-Eu(1)-O(7)	142.61(12)
O(1)-Eu(1)-O(3)#2	77.21(12)	O(1)-Eu(1)-O(8)#2	87.43(12)
O(2)#1-Eu(1)-O(3)#2	147.06(12)	O(5)-Eu(1)-O(3)#2	122.27(12)
O(2)#1-Eu(1)-O(4)#2	156.38(14)	O(5)-Eu(1)-O(6)#3	134.11(12)
O(2)#1-Eu(1)-O(5)	80.32(12)	O(6)#3-Eu(1)-O(3)#2	75.99(12)
O(2)#1-Eu(1)-O(6)#3	106.50(13)	O(7)-Eu(1)-O(3)#2	129.82(12)
O(2)#1-Eu(1)-O(7)	79.23(12)	O(7)-Eu(1)-O(4)#2	89.95(13)
O(2)#1-Eu(1)-O(8)#3	77.52(12)	O(8)#3-Eu(1)-O(4)#2	125.62(13)
O(4)#2-Eu(1)-O(3)#2	53.17(12)	O(8)#3-Eu(1)-O(5)	153.49(12)
O(4)#2-Eu(1)-O(5)	76.12(13)	O(8)#3-Eu(1)-O(6)#3	67.18(12)

#1 -x,1-y,1-z; #2 1-x,1-y,1-z; #3 +x,3/2-y,-1/2+z; #4 +x,3/2-y,1/2+z

Complex 2			
Gd(1)-O(1)	2.295(4)	Gd(1)-O(5)#4	2.421(4)
Gd(1)-O(2)#1	2.358(4)	Gd(1)-O(6)#3	2.415(4)
Gd(1)-O(3)#2	2.470(4)	Gd(1)-O(7)	2.380(4)
Gd(1)-O(4)#2	2.404(4)	Gd(1)-O(8)#3	2.400(4)
O(1)-Gd(1)-O(2)#1	86.74(14)	O(4)#2-Gd(1)-O(3)#2	53.40(14)
O(1)-Gd(1)-O(3)#2	77.31(14)	O(4)#2-Gd(1)-O(5)	75.93(14)
O(1)-Gd(1)-O(4)#2	89.50(16)	O(4)#2-Gd(1)-O(6)#3	89.40(16)
O(1)-Gd(1)-O(5)	76.31(14)	O(5)-Gd(1)-O(3)#2	122.10(14)
O(1)-Gd(1)-O(6)#3	147.05(14)	O(2)#1-Gd(1)-O(6)#3	106.22(14)
O(1)-Gd(1)-O(7)	142.71(14)	O(2)#1-Gd(1)-O(7)	79.65(14)
O(1)-Gd(1)-O(8)#3	87.02(14)	O(2)#1-Gd(1)-O(8)#3	77.31(14)
O(2)#1-Gd(1)-O(3)#2	146.95(14)	O(6)#3-Gd(1)-O(3)#2	75.89(14)
O(2)#1-Gd(1)-O(4)#2	156.33(15)	O(6)#3-Gd(1)-O(5)	134.91(13)
O(2)#1-Gd(1)-O(5)	80.48(14)	O(7)-Gd(1)-O(3)#2	129.45(15)
O(7)-Gd(1)-O(4)#2	89.45(15)	O(8)#3-Gd(1)-O(3)#2	73.26(13)
O(7)-Gd(1)-O(5)	67.31(13)	O(8)#3-Gd(1)-O(4)#2	125.85(15)

O(7)-Gd(1)-O(6)#3	70.20(13)	O(8)#3-Gd(1)-O(5)	152.88(14)
#1 -x,1-y,1-z; #2 1-x,1-y,1-z; #3 +x,3/2-y,-1/2+z; #4 +x,3/2-y,1/2+z			
Complex 3			
Eu(1)-O(1)	2.382(3)	O(4)#2-Eu(1)-O(1)#1	124.97(8)
Eu(1)-O(1)#1	2.837(3)	O(5)-Eu(1)-O(1)#1	114.83(8)
Eu(1)-O(2)#1	2.470(2)	O(5)-Eu(1)-O(2)#1	78.80(9)
Eu(1)-O(3)#2	2.464(2)	O(5)-Eu(1)-O(3)#2	85.72(9)
Eu(1)-O(4)#2	2.518(3)	O(5)-Eu(1)-O(4)#2	75.85(9)
Eu(1)-O(5)	2.425(3)	O(5)-Eu(1)-O(6)#3	67.08(9)
Eu(1)-O(6)#3	2.429(3)	O(5)-Eu(1)-O(7)	68.75(9)
Eu(1)-O(7)	2.452(3)	O(6)#3-Eu(1)-O(1)#1	66.61(8)
Eu(1)-O(8)	2.367(3)	O(6)#3-Eu(1)-O(2)#1	77.68(9)
O(1)-Eu(1)-O(1)#1	65.69(9)	O(6)#3-Eu(1)-O(3)#2	121.45(9)
O(1)-Eu(1)-O(2)#1	113.96(9)	O(6)#3-Eu(1)-O(4)#2	70.43(8)
O(1)-Eu(1)-O(3)#2	94.91(9)	O(7)-Eu(1)-O(1)#1	116.75(8)
O(1)-Eu(1)-O(4)#2	76.24(9)	O(7)-Eu(1)-O(2)#1	74.24(9)
O(1)-Eu(1)-O(5)	144.06(9)	O(7)-Eu(1)-O(3)#2	74.14(9)
O(1)-Eu(1)-O(6)#3	82.48(9)	O(7)-Eu(1)-O(4)#2	117.13(9)
O(1)-Eu(1)-O(7)	145.76(9)	O(8)-Eu(1)-O(1)	72.45(10)
O(2)#1-Eu(1)-O(2)#1	48.53(9)	O(8)-Eu(1)-O(1)#1	74.23(8)
O(2)#1-Eu(1)-O(4)#2	145.00(9)	O(8)-Eu(1)-O(2)#1	84.10(9)
O(3)#2-Eu(1)-O(1)#1	158.84(9)	O(8)-Eu(1)-O(3)#2	92.41(9)
O(3)#2-Eu(1)-O(2)#1	148.06(10)	O(8)-Eu(1)-O(4)#2	130.00(9)
O(3)#2-Eu(1)-O(4)#2	52.56(9)	O(8)-Eu(1)-O(5)	143.49(10)
#1 1-x,-y,2-z; #2 1-x,1-y,1-z; #3 2-x,-y,2-z			
Complex 4			
Gd(1)-O(1)	2.365(3)	O(4)#2-Gd(1)-O(1)#1	158.25(8)
Gd(1)-O(1)#1	2.859(3)	O(4)#2-Gd(1)-O(2)#1	148.73(9)
Gd(1)-O(2)#1	2.455(3)	O(4)#2-Gd(1)-O(3)#2	52.79(9)
Gd(1)-O(3)#2	2.503(3)	O(5)-Gd(1)-O(1)#1	114.83(9)

Gd(1)-O(4)#2	2.499(3)	O(5)-Gd(1)-O(3)#2	75.93(9)
Gd(1)-O(5)	2.402(3)	O(5)-Gd(1)-O(6)#3	67.49(9)
Gd(1)-O(6)#3	2.415(3)	O(5)-Gd(1)-O(7)	68.55(10)
Gd(1)-O(7)	2.438(3)	O(6)#3-Gd(1)-O(1)#1	66.21(9)
Gd(1)-O(8)	2.346(3)	O(6)#3-Gd(1)-O(3)#2	70.47(10)
O(1)-Gd(1)-O(1)#1	65.60(10)	O(6)#3-Gd(1)-O(4)#2	121.93(10)
O(1)-Gd(1)-O(2)#1	113.55(10)	O(6)#3-Gd(1)-O(7)	131.24(9)
O(1)-Gd(1)-O(3)#2	76.27(10)	O(7)-Gd(1)-O(1)#1	116.82(9)
O(1)-Gd(1)-O(4)#2	94.49(9)	O(7)-Gd(1)-O(2)#1	74.49(9)
O(1)-Gd(1)-O(5)	144.23(10)	O(7)-Gd(1)-O(3)#2	117.24(10)
O(1)-Gd(1)-O(6)#3	82.26(9)	O(7)-Gd(1)-O(4)#2	74.46(9)
O(1)-Gd(1)-O(7)	145.82(10)	O(8)-Gd(1)-O(1)#1	73.81(9)
O(2)#1-Gd(1)-O(1)#1	48.23(8)	O(8)-Gd(1)-O(1)	72.32(9)
O(2)#1-Gd(1)-O(3)#2	144.92(10)	O(8)-Gd(1)-O(3)#2	130.45(9)
O(3)#2-Gd(1)-O(1)#1	124.74(9)	O(8)-Gd(1)-O(4)#2	92.49(10)
#1 1-x,-y,2-z; #2 1-x,1-y,1-z; #3 2-x,-y,2-z			

Table S3. Ions leading to fluorescence sensing for **3** in different organic solvents.

Organic solvents	metal ions	Inorganic anions
DMF	Fe ³⁺ Cu ²⁺	Cr ₂ O ₇ ²⁻
DMA	Fe ³⁺ Cu ²⁺	Cr ₂ O ₇ ²⁻
EtOH	Fe ³⁺ Cu ²⁺	--
MeOH	Fe ³⁺ Cu ²⁺	--
CH ₃ CN	Fe ³⁺ Cu ²⁺	--